sciendo

Studia Geotechnica et Mechanica, 2023; 45(1): 41–54

Original Study

Open Access

Djamal Yahmi[1,*], Taïeb Branci[2], Abdelhamid Bouchaïr[3], Eric Fournely[3]

Overstrength and ductility factors of XBF structures with pinned and fixed supports

https://doi.org/10.2478/sgem-2022-0028
received November 8, 2021; accepted November 14, 2022.

Abstract: In today's time, most seismic design codes are based on a linear elastic force-based approach that includes the nonlinear response (ductility and overstrength) of the structure through a reduction factor (named behavior factor q in Eurocode 8 [EC8]). However, the use of a prescribed q-factor that is constant for a given structural system may fail in providing structures with the same risk level. This paper focuses on the estimation of actual values of q-factor for X-braced steel frames (XBFs) designed according to the European codes and comparing these values to those suggested in EC8. For this purpose, a nonlinear pushover analysis has been performed. The effects of specific parameters, such as the stories number, the brace slenderness ratio, the local response of structural members, and the support type, are evaluated. The results show that the most important parameter that affects the q-factor is the brace slenderness ratio, while the support type has less effect on this factor. Furthermore, a local strength criterion has been proposed to implicitly ensure that the suggested value of the q-factor is conservative.

Keywords: Behavior factor; Overstrength; Ductility; X-braced steel frames; Eurocode 8.

1 Introduction

Currently, the reduction factor is widely used in most of the seismic design codes, trying to compensate the effects of significant overstrength and ductility of the structure to withstand seismic load. In other words, design codes allow simplified elastic analysis to be performed, calculating the design forces acting on the structure from spectra based on linear behavior and properly scaled down by a suitable reduction factor that accounts for the global nonlinear effects. The reduction factor is called behavior factor (q-factor) in Eurocode 8 (EC8) [1] and response modification factor (R-factor) in Uniform Building Code [2]. Here, the European term will be used, since this study is mainly focused on the European seismic design practice. Based on the elastic analysis, EC8 gives a constant value of q-factor for all structures with a specific structural system, regardless of the own structural characteristics. However, in reality, a change in the structural characteristics, as dimensions of structural members and height of building, has a direct effect on the dissipation energy of the structural system [3, 4, 5], which influences the q-factor value. This may lead to q-factor value not always on the conservative side compared to the actual dissipative features of the structure [5].

Previous studies were conducted in order to define the parameters affecting the q-factor value of concentrically braced frames [6-11]. Some of these parameters include type of bracing system, bay lengths, and type of connections between structural members. It has been recognized that there are other parameters which may influence the q-factor value for other structural typology with different ductility classes requiring more detailed investigations. In this context, the present research proposes investigating the influence of the parameters stories number, brace slenderness ratio, local response of structural members (braces), and support type on the q-factor value of X-braced steel frames (XBFs) designed according to European codes [1, 12]. The q-factor components (overstrength and ductility) are evaluated using pushover analysis.

2 EC8 design criteria for XBFs

Concentric X-braced system (XBF) is known to be a very effective structural element that can provide lateral stiffness and strength in steel building structures. This

***Corresponding author: Djamal Yahmi,** Djilali Bounaama University of Khemis Miliana, Khemis Miliana, Algeria, E-mail: d.yahmi@univ-dbkm.dz
Taïeb Branci, Hassiba Benbouali University of Chlef, Chlef, Algeria
Abdelhamid Bouchaïr, Eric Fournely, Clermont Auvergne INP, CNRS, Institut Pascal, Université Clermont Auvergne, F-63000 Clermont-Ferrand, France

system is used as lateral (i.e., seismic and wind) force resisting system through the vertical concentric truss system [13]. In XBF structures, according to EC8, braces are the dissipative members, while all the other members (i.e., beams and columns) should remain elastic. The braces act as fuses which dissipate the input seismic energy through axial deformations in tension and compression loading cycles. Hereafter, the main design rules of the EC8 for seismic resistant systems with X-braces are summarized.

Firstly, the slenderness ratio of braces members should be limited to $1.3 \leq \lambda \leq 2.0$, where the upper limit has the aim to avoid excessive distortions due to buckling of braces in compression, which could cause damage to connections, while the lower limit ensures the validity of the structural model with only active tensile braces as well as restricts the design internal forces in the columns. Moreover, a special rule is presented in EC8 to ensure homogeneous dissipative behavior of braces along the height of a structure. According to EC8, the overstrength of a brace member Ω_i is calculated as follows:

$$\Omega_i = N_{pl,Rd,i} / N_{Ed,i} \tag{1}$$

where $N_{pl,Rd,i}$ is the design plastic resistance of the brace i and $N_{Ed,i}$ the design axial force in the brace i in the seismic design situation. EC8 mandates that the maximum overstrength shall not differ from the minimum by more than 25%. Thus,

$$\Omega_i^{max} / \Omega_i^{min} \leq 1.25 \tag{2}$$

Based on EC8, XBF structures are classified into three categories and the *q*-factor changes depending on this category. Two broad categories are defined: low dissipative structural behavior and dissipative structural behavior. Low dissipative structural behavior corresponds to ductility class low, where the recommended value of *q*-factor is equal to 1.5. Dissipative structural behavior is subdivided into two categories, namely, ductility class medium and ductility class high, where the recommended value of *q*-factor is 4.0, regardless of the ductility class.

Thus, it can be seen clearly that the EC8 does not give enough precision about the effect of structural characteristics (stories number, brace slenderness ratio, local response of structural members, and support type) on the *q*-factor. The effect of these parameters on the value of *q*-factor is an essential and pressing objective of this study.

3 Literature review

Nowadays, the linear elastic design method is commonly used in most seismic codes. In this method, the most important parameter is the *q*-factor, which plays a paramount role in designing the earthquake load-resisting elements. Because of the importance of *q*-factor on the dynamic response of structure and its relationship with the overstrength and ductility factors, the parameters that affect this factor have been an important research topic for the last few decades [14-17].

The effect of vibration period on the nonlinear response of frame is of major interest, in particular, on the components of *q*-factor. According to Osteraas and Krawinkler [14], the overstrength factor of steel frames was observed on steel moment-resisting frames (SMRFs), with various bay sizes and heights, using a pushover analysis. The authors found that the overstrength factor ranged from 8.0 at a short period to 2.1 at a period of 4.0 s. Rahgozar and Humar [15] determined the overstrength factor of concentrically braced steel frames (CBFs) from 2 to 30 stories and showed that this factor is almost independent of the height of the frame. Mahmoudi and Zaree [8] also determined the overstrength of CBFs. They observed that the height of frame makes a slight difference in terms of redundancy factor (R_ρ-factor), while it shows a significant effect on the design overstrength factor (R_Ω-factor). Moreover, in order to assess the effect of beams–columns semi-rigid connections on the *q*-factor components of steel frames, Balendra and Huang [6] studied SMRFs with three, six, and nine stories having rigid and semi-rigid beam–column connections. The results indicated that the frames with semi-rigid connections have a lower overstrength reaching 50% that of frames with rigid connections. Performing nonlinear static pushover analyses, Kim and Choi [7] determined the *q*-factor of concentric chevron-braced steel frames with different stories number and bay lengths. The authors showed that the *q*-factor components increased as the structure height decreased and the bay length increased. Fanaie and Dizaj [16] also studied the effect of stories number on the *q*-factor components, considering buckling-restrained braced frames. The results indicated that the overstrength and ductility factors decrease as the number of stories increases. Faggiano et al. [9] performed pushover analysis on CBFs designed according to the Italian code to estimate their *q*-factors. The authors found that the Italian code recommends a lower-than-actual value of *q*-factor. Fanaie and Shamlou [10] elaborated a study to assess the *q*-factor of mixed structures combining reinforced concrete frames and shear walls in the lower

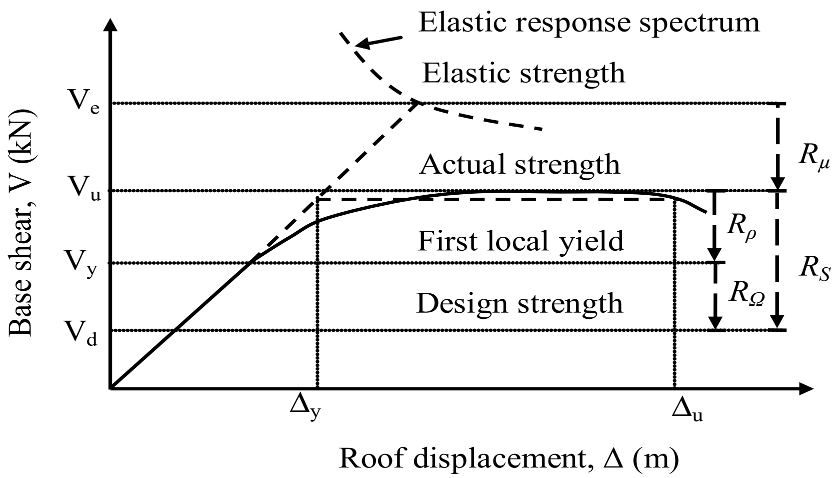

Figure 1: Base shear versus roof displacement relationship [5, 22].

stories and steel frames with bracing in the upper stories. The results showed that, the *q*-factors of mixed structures are lower than those of steel or concrete structures with the same heights. A study was performed by Attia and Irheem [17] on overstrength, ductility, and behavior factor of X-braced steel structures with different column strong axis orientations, bay number, and stories number. They found that the most important parameter that affects the *q*-factor value is the column orientation. The effect of other parameters was minor.

These studies did not consider the effect of "brace slenderness ratio" and local response of the braces on the *q*-factor, especially for XBFs. Also, although several studies have been conducted on the influence of stories number on the *q*-factor, it remains of big interest to clarify its effect on *q*-factor for different structural systems and ductility classes of structures. A detailed methodology for the computation of *q*-factor is presented hereafter.

4 Methods for evaluating behavior factor

Clear definitions of the *q*-factor are difficult to find in seismic codes, but it is almost generally accepted that this factor simply represents the ratio of the elastic strength demand, that is, the strength that would be required in the structure, if it were to respond elastically to the design earthquake, to the inelastic strength demand, that is, the strength required in the structure for it to respond beyond the elastic range, but within the selected ductility (and/or displacement) limits [18]. Mazzolani and Piluso [19] addressed various theoretical procedures to compute the *q*-factor, such as the maximum plastic deformation approach and the energy approach. The formulation of the *q*-factor proposed by Applied Technology Council (ATC)-34 [20] is the most used currently [5, 21]. It is expressed as the product of three parameters that significantly influence the seismic response of structures. For this study, the evaluation of *q*-factor is made by means of the nonlinear static procedure (capacity curve, see Fig. 1) using the formulation of ATC-34. Hence, the *q*-factor (*R*-factor in ATC) is defined as

$$R = R_S \cdot R_\mu \cdot R_\zeta \tag{3}$$

In Eq. (3), R_S is the overstrength factor, R_μ is the ductility factor, and R_ζ is the damping factor. R_ζ is typically set equal to 1.0, as, in general, it is assumed that the damping ratio is the same for both linear and nonlinear systems [5]. The assessment of R_S- and R_μ-factors can be obtained from the capacity curve represented by the relationship between the base shear force and the roof lateral displacement (see Fig. 1).

Observations during earthquakes have shown that building structures could take the forces considerably larger than those that they were designed for. This is explained by the presence in such structures of significant overstrength not accounted for in design. The main possible sources of overstrength that have been reviewed by Rahgozar and Humar [15] include the difference between the actual and the design material strength, the effect of minimum requirements on member sections in order to meet the stability and serviceability limits, and the redistribution of internal forces. The presence of the overstrength R_S-factor in structures may be classified into two categories [3, 5, 8]: the design overstrength (R_Ω-factor) and the redundancy (R_ρ-factor). The R_S-factor is generally expressed as follows:

$$R_S = \frac{V_u}{V_d} = \frac{V_y}{V_d} \cdot \frac{V_u}{V_y} = R_\Omega \cdot R_\rho \tag{4}$$

where V_u, V_y, and V_d correspond to the ultimate strength, the first significant yield strength, and the design strength, respectively.

The displacement ductility μ is a measure of the global nonlinear response of a structure and is commonly used to represent the capacity of a structure to dissipate energy. It can be taken into account through the R_μ-factor. It is particularly important for steel structures since the beneficial effect of ductility is supposed to come from different sources in such structures [23]. In the last three decades, several studies have focused on the evaluation of the R_μ-factor. The works by Nassar and Krawinkler [24] and Fajfar [25] are significant and are frequently referred to. The authors developed relationships for the determination of ductility factor by relating the R_μ and μ parameters. In this study, the most used relationships [3, 26] developed by Fajfar [25] are used to calculate the R_μ-factor. Thus,

$$R_\mu = (\mu - 1)\frac{T}{T_C} + 1 \ for\ T < T_C \tag{5}$$

$$R_\mu = \mu \ for\ T \geq T_C \tag{6}$$

where T is the vibration fundamental period of the structure and T_c is the characteristic period of ground motion. μ is defined as the ratio of the ultimate displacement Δ_u, corresponding to the selected performance level of failure, and the yield displacement Δ_y of the structure. This ratio is given by Eq. (7) as follows:

$$\mu = \frac{\Delta_u}{\Delta_y} \tag{7}$$

Yield displacement is judged through an idealization of base shear force versus roof lateral displacement relationship (pushover or capacity curve). For this purpose, a bilinear curve is fitted to the capacity curve using an elastic, perfectly plastic shape. The initial stiffness of the idealized curve is determined in such a way that the areas under the actual and idealized capacity curves are the same [1].

In the EC8 [1], the q-factor for steel structures is defined as follows:

$$q = q_0 \frac{\alpha_u}{\alpha_1} \tag{8}$$

in which q_0 is the basic value of the behavior factor and the a_u/a_1 ratio is the redundancy factor. A comparison between Eq. (3) and Eq. (8) leads to $\alpha_u/\alpha_1 = R_\rho$ and $q_0 = R_\mu R_\Omega$ [5].

The approach presented above is commonly used to obtain the q-factor from the capacity curve represented by the relationship between the base shear force and the roof displacement.

5 Numerical analysis

Based on the existing studies [3, 5, 27, 28], the structural response curve (capacity curve) is obtained by two different methods of analysis: the nonlinear static pushover analysis (NSPA) and the nonlinear dynamic analysis. The first method is simple to use and gives accurate results. It is chosen in the present study.

5.1 Data assumed for the studied structures

In the current work, a number of XBFs having three, six, and nine stories and three bays of 6 m each with a height of 3 m for each floor (Fig. 2) are analyzed to evaluate the impact of various parameters on the q-factor. These frames have been designed according to the European codes [1, 12] on the basis of a peak ground acceleration equal to 0.35 g, damping coefficient ξ = 5%, soil class B, and behavior factor q_{design} = 4.0. Gravity load on the beams is assumed to be equal to 27.5 kN/m (dead and live loads of floors), while steel members are made of grade S235. Data of the frames are presented in Table 1 taken from Kamaris et al. [29]. The beam sections consist of standard IPE300 sections. The profiles used for the braces are circular tubular sections (TUBO). The columns are pinned at their bases (and fixed in the second case), while beam-to-column and brace-to-beam connections are hinged.

For each frame corresponding to a stories number (three, six, or nine stories), three design processes were performed in order to obtain three distinct values (1.93, 1.56, and 1.30) of the brace slenderness ratio, λ_i, defined as

$$\lambda_i = \frac{l}{\pi \cdot r}\sqrt{\frac{f_y}{E}} \tag{9}$$

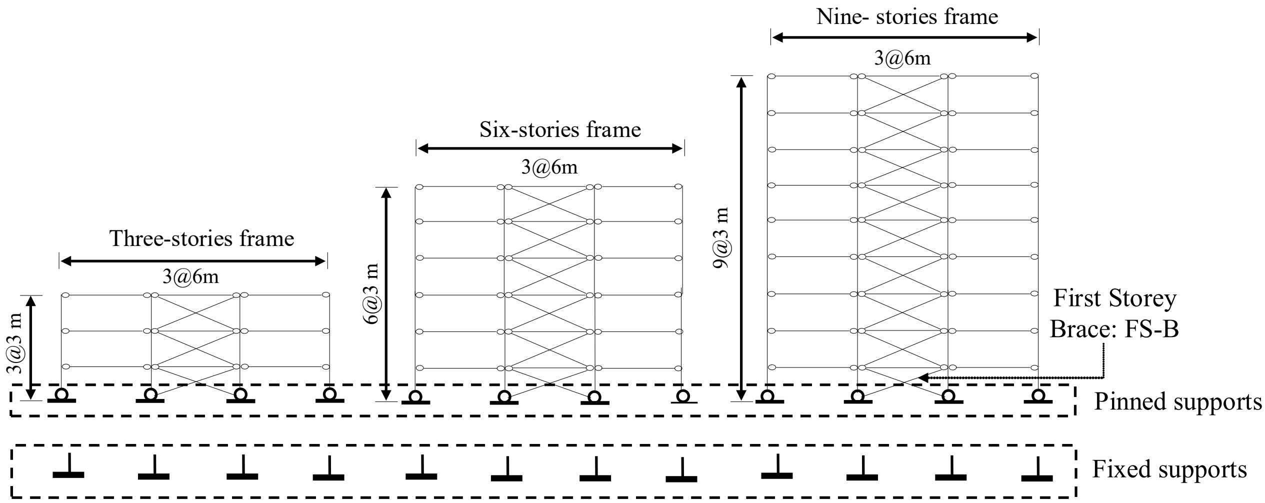

Figure 2: Studied frames.

Table 1: XBF steel structures considered in parametric studies.

Storey number	λ_i	Columns: HEB (N° of storey)	Braces: TUBO (N° of storey)
Three stories	$\lambda_1 = 1.93$	220 (1–3)	127X4 (1) + 108X3.6 (2) + 101.6X3.6 (3)
	$\lambda_2 = 1.56$	240 (1–3)	152.4X4 (1) + 133X4 (2) + 127X4 (3)
	$\lambda_3 = 1.30$	260 (1–3)	193.7X4.5 (1) + 159X4 (2) + 139.7X4 (3)
Six stories	$\lambda_1 = 1.93$	240 (1–2) + 220 (3–4) + 200 (5–6)	127X4 (1–3) + 108X3.6 (4) + 101.6X3.6 (5) + 82.5X3.2 (6)
	$\lambda_2 = 1.56$	260 (1–2) + 240 (3–4) + 220 (5–6)	152.4X4 (1–2) + 139.7X4 (3) + 133X4 (4) + 127X4(5) + 101.6X3.6 (6)
	$\lambda_3 = 1.30$	280 (1–2) + 260 (3–4) + 240 (5–6)	193.7X4.5 (1–2) + 168.3X4 (3) + 159X4 (4) + 139.7X4(5) + 127X4 (6)
Nine stories	$\lambda_1 = 1.93$	260 (1–3) + 240 (4–6) + 220 (7–9)	127X4 (1–4) + 108X3.6 (5–6) + 101.6X3.6 (7) + 88.9X3.2 (8) + 76.1X3.2 (9)
	$\lambda_2 = 1.56$	280 (1–3) + 260 (4–6) + 240 (7–9)	152.4X4 (1–3) + 139.7X4 (4) + 133X4 (5) + 127X4 (6–7) + 108X3.6 (8) + 88.9X3.2 (9)
	$\lambda_3 = 1.30$	320 (1–3) + 300 (4–6) + 280 (7–9)	193.7X4.5 (1–4) + 159X4 (5) + 152.4X4 (6) + 139.7X4 (7) + 127X4 (8) + 108X3.6 (9)

Table 2: Modal periods and mass ratios of the analyzed XBF steel structures.

Storey number	λ_i	T_1 (s)	T_2 (s)	T_3 (s)	M^{*1}	M^{*2}	M^{*3}	V_d/W
Three stories	$\lambda_1 = 1.93$	0.41	0.14	0.09	0.86	0.11	0.02	0.22
	$\lambda_2 = 1.56$	0.36	0.13	0.08	0.87	0.10	0.02	0.23
	$\lambda_3 = 1.30$	0.32	0.11	0.07	0.85	0.12	0.02	0.23
Six stories	$\lambda_1 = 1.93$	0.83	0.28	0.16	0.78	0.15	0.03	0.13
	$\lambda_2 = 1.56$	0.75	0.25	0.14	0.79	0.15	0.03	0.14
	$\lambda_3 = 1.30$	0.68	0.22	0.12	0.77	0.16	0.04	0.16
Nine stories	$\lambda_1 = 1.93$	1.37	0.44	0.24	0.75	0.17	0.04	0.08
	$\lambda_2 = 1.56$	1.24	0.40	0.22	0.76	0.17	0.04	0.09
	$\lambda_3 = 1.30$	1.10	0.34	0.19	0.75	0.19	0.04	0.10

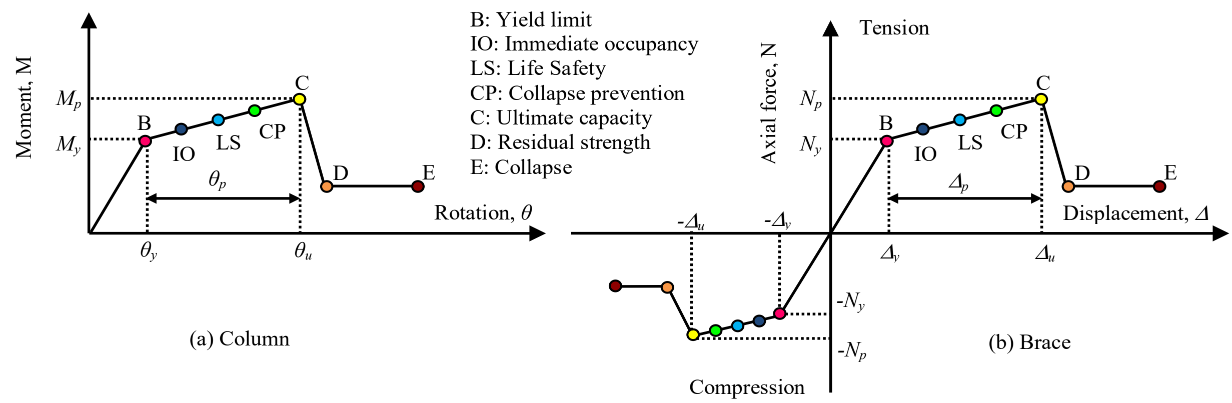

Figure 3: Plastic hinges of a cross section [32].

where l is the buckling length, r is the radius of gyration of the cross section, f_y is the yield strength of the material, and E is Young's modulus. The parameter λ_i varies along the height of the frame, and therefore, its nominal value was calculated for the storey closest to the mid-height of the structure.

Table 2 presents the natural periods and the modal mass ratios M^{*1}, M^{*2}, M^{*3} of the first three mode shapes of the dynamic modal analysis, where it can be observed that the total mass participating in the fundamental mode of the studied frames is higher than 75%. This allows using the NSPA, which is mainly based on the fundamental mode.

5.2 Modeling approach for inelastic analysis

Analyses have been performed using the finite element software SAP2000 [30], which is a general-purpose structural analysis program for static and dynamic analyses of structures. In this study, SAP2000 Nonlinear Version 14 has been used. A description of the modeling details is provided in the following.

A two-dimensional finite element model of each frame structure is created in SAP2000 to perform NSPA. Structural members are modeled as beam elements with lumped plasticity. Plastic hinges of columns and beams are assigned to the end of the members, while for modeling the nonlinear behavior of braces, the plastic hinges are defined at the midpoint of each brace. Moreover, for columns, the effect of the axial load is considered using a model of P–M interaction diagram (axial force P and bending moment M). The plastic hinge properties in SAP2000 are determined according to the provisions of FEMA 356 [31] (Fig. 3).

In this analysis, the geometric and mechanical characteristics of steel members are considered. Also, all sources of geometrical nonlinearity have been included, namely P-delta and large displacement effects. The analysis of XBF structures is performed by considering only the contribution of braces in tension, assuming that at collapse, braces in compression are already buckled and do not provide any bearing capability.

The frames are subjected to two horizontal load patterns, a uniform pattern UD, whereby lateral forces are proportional to the total mass at each floor level, and an inverted triangular pattern TD, in which seismic forces are proportional to the product of floor mass and storey height [32, 33, 34]. The horizontal loads are distributed along the frame height with the intensity increased incrementally until a mechanism is reached. It leads to construct the capacity curve, which is used to obtain the q-factor components.

5.3 Validation of capacity curve

In this investigation, the capacity curve plotted using DRAIN-2DX computer program of six-storey steel frame studied by Karavasilis et al. [35] was used to validate the capacity curve obtained by SAP2000 [30]. The considered frame has three bays of 6 m each and storey height equal to 3 m. The first three stories have columns with HEB340 sections and beams with IPE450 sections, whereas the last three (upper) stories have columns with HEB280 sections and beams with IPE360 sections. Steel members are made of grade S235. The comparison between the two curves represented in Fig. 4 shows that the two curves are very close.

6 Results and discussion

The numerical results of the studied XBFs are presented and discussed in this section. NSPA using inverted TD and UD load pattern distribution was carried out to compute the q-factor components, such as the overstrength R_S and ductility R_μ factors. The effects of brace slenderness ratio λi, stories number, local response of structural members (braces), and support type on the q-factor were investigated.

In Fig. 5, the capacity curves of the studied XBF structures with the three values of brace slenderness ratio (λ_1, λ_2, and λ_3) for the two types of supports (pinned and fixed supports) are depicted. The section damage levels of the first-storey brace (FS-B) are marked on the capacity curve (FS-B). It can be seen that the brace slenderness ratio, λ_i, does not make any major difference in terms of lateral displacement. However, this parameter has a significant influence on the base shear force. The base shear force obtained for the frames with $\lambda_3 = 1.30$ is greater than that of those with $\lambda_1 = 1.93$ and $\lambda_2 = 1.56$. This is due to the increase in the dimensions of braces' cross sections (hence, an increase in their axial capacity), which will absorb more forces. For such frames (especially for nine-storey frame), greater differences have been found between the results obtained from NSPA under UD and TD. The outcome of the present study is in good agreement with the numerical work reported by Ferraioli et al. [5]. Besides, Fig. 5 indicates that the risk of local brace instability, due to the loss of rigidity after reaching the ultimate capacity (point C in Fig. 3), increases as the number of stories increases. Moreover, for such frames, the FS-B section is the first and the most damaged section, which leads to a premature failure of the frame. The appearance of such premature failure (soft-storey mechanism) confirms the importance of design methods focusing on the performance-based plastic design (PBPD) of steel frame structures [36, 37].

Figs 6 and 7 show the distribution of plastic hinges for the studied frames with $\lambda_1 = 1.93$ (the maximum value of brace slenderness ratio). It appears that there is a good distribution of energy dissipation along the height and across the length of low-rise frames (three stories). However, for medium (six stories) and high-rise frames (nine stories), the ultimate capacity is reached in the plastic hinge of FS-Bs, while those on the top of the frame remain in the elastic domain without plastic dissipation. This is due to the concentration of high axial force at the FS-Bs' sections. Furthermore, in the case of the frames with fixed supports (λ_1'), it is observed that the plastic hinges are formed also at the first-storey column sections in all the frames (three, six, and nine stories). This distribution

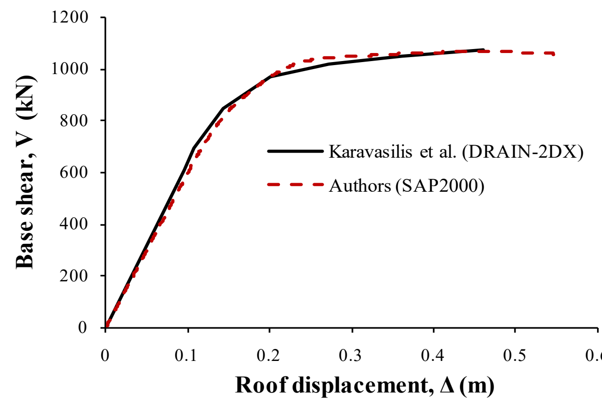

Figure 4: Capacity curves of the analyzed six stories steel frame.

could be explained by the sensitivity of the frames to the P-delta effect, which is influenced by the large lateral displacement and the high value of axial force.

In order to compute the q-factor components, capacity curves of the studied XBF structures are obtained from NSPA. However, relevant information collected from the plot must first be idealized. Bilinear idealization provides the main parameters which are significant yield base shear and displacement, as well as predetermined base shear force and ultimate displacement related to the failure mode of the structure (Fig. 1). The R_S- and R_μ-factors are calculated as discussed in section 4. The following sections discuss the results of computing q-factor, considering the effects of structural characteristics and brace slenderness ratio.

6.1 Structural characteristics' effects on the *q*-factor

Fig. 8 shows the variation of the q-factor components under the effects of stories number and support type (pinned and fixed supports). They have to be multiplied together to get the global behavior factor. In particular, the R_S- and R_μ-factors resulting from NSPA using two lateral load patterns distribution (inverted TD and UD) are shown.

In Fig. 8, it can be noticed that the number of stories influences the R_S-factor. The greater value of this factor is obtained for low-rise frames. This result could be explained by the fact that the magnitude of overstrength depends on the relative ratio between the gravity and the earthquake loads. Comparison between the earthquake base shear and the total gravity load ratio of the studied frames (see Table 2) shows that the highest V_d/W ratio is observed for three-storey frame, reflecting the high

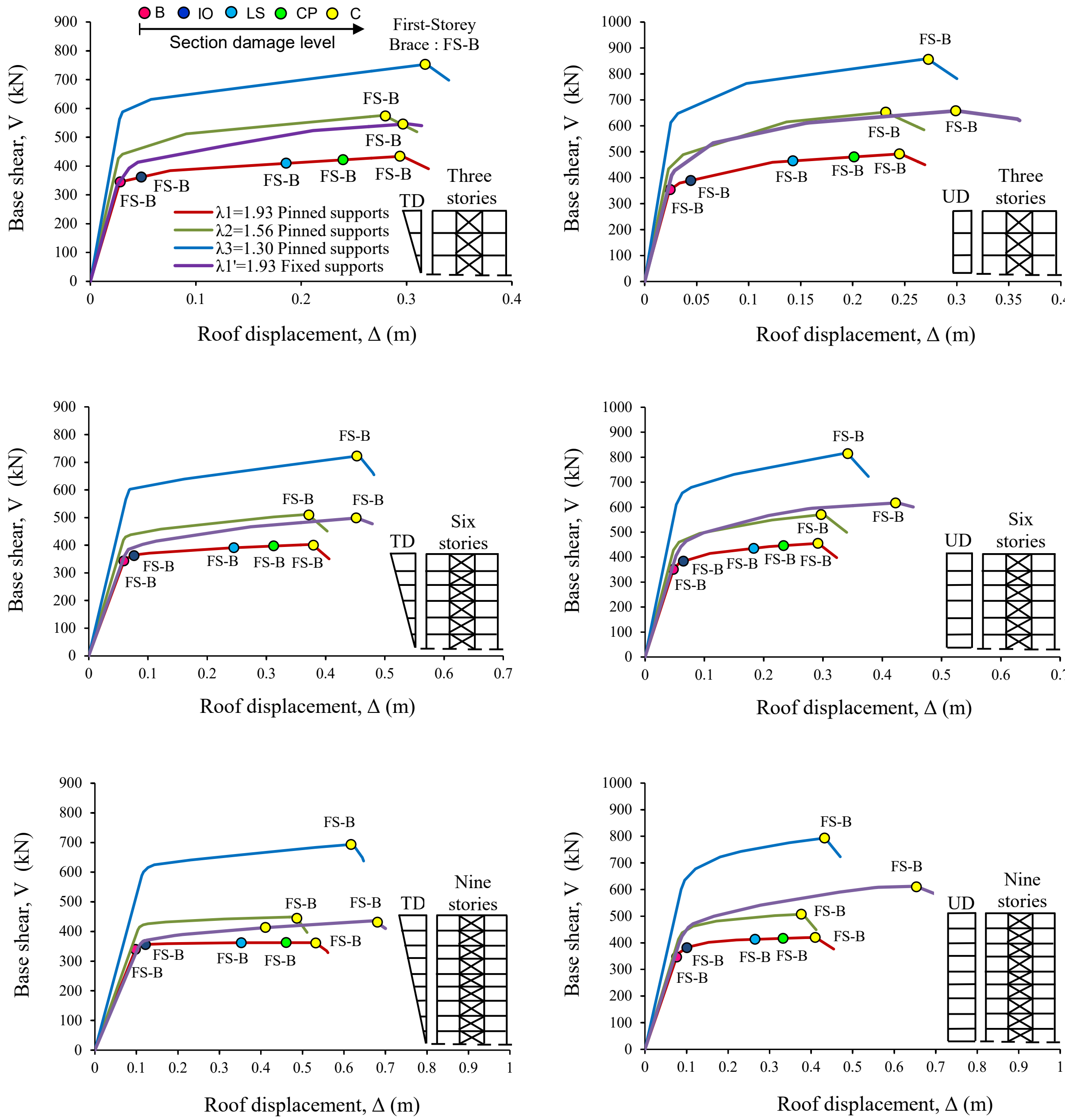

Figure 5: Capacity curves of the analyzed frames.

stiffness and efficiency of this frame in resisting lateral forces. The lowest V_d/W ratio is observed for nine-storey frame as a result of the high total gravity load. Moreover, the greatest values of R_S-factor are obtained under UD lateral loading.

The R_μ-factor is obtained from the idealized capacity curve. In the light of the obtained results (Fig. 8), it can be seen that the R_μ-factor is almost constant regardless of the number of stories. It can also be observed that the values of the R_μ-factor obtained under the inverted TD are higher than the ones obtained under UD lateral loading.

Fig. 8 also shows the variation of the calculated q-factors as a function of the number of stories and the load patterns. The q-factor value specified by EC8 is represented by a horizontal line (q_{design} = 4 for XBF steel structures). In general, the number of stories has a significant influence on the q-factor. It is clear that the value of q-factor decreases as the number of stories

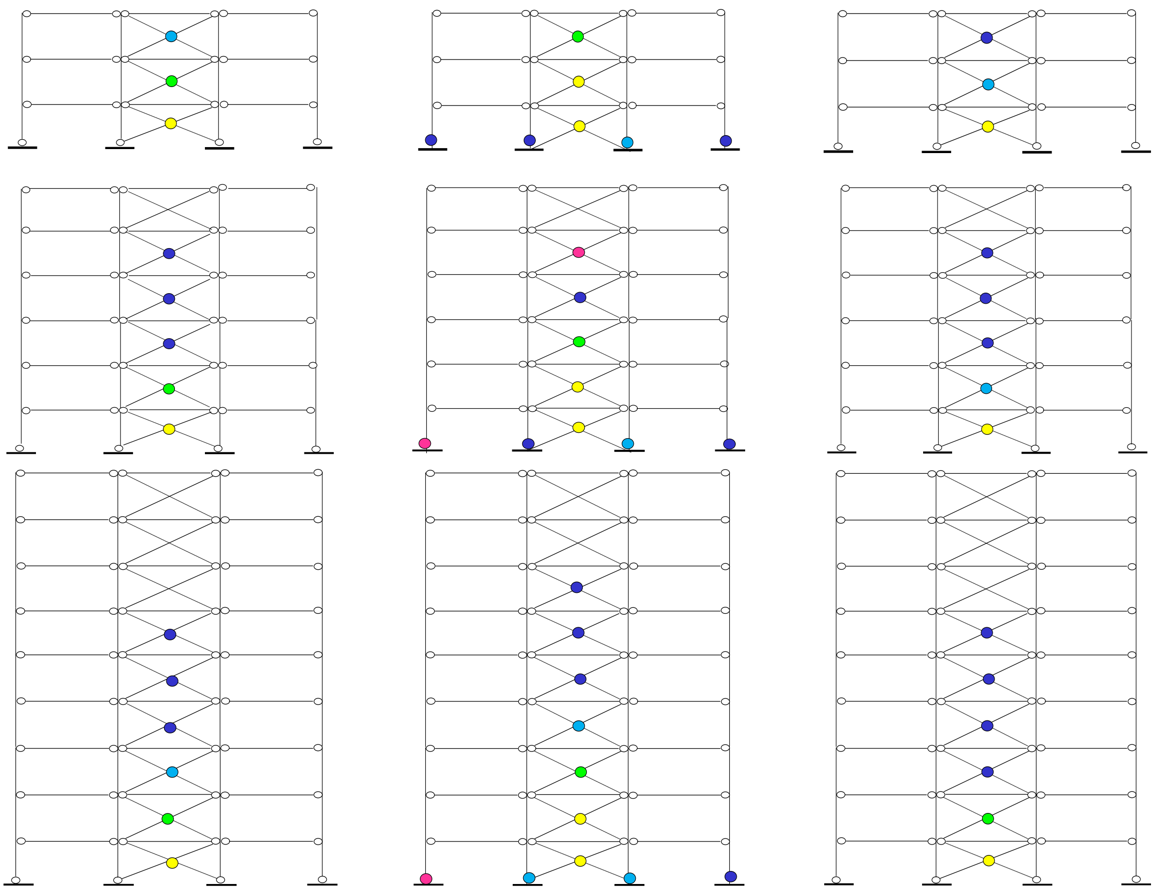

TD (λ_1) – Pinned supports TD (λ_1’) – Fixed supports UD (λ_1) – Pinned supports

Figure 6: Plastic hinges’ distribution of the studied frames with $\lambda_1 = 1.93$.

increases. The outcome of this research work is in perfect concordance with the findings of Ferraioli et al. [5] and Branci et al. [38], where they found that the *q*-factor increases gradually with a decrease in the height of building (stories number). Moreover, for such frames, small differences have been found between the *q*-factor values obtained under TD and UD. This is due to the occurrence of local plastic mechanisms of the braces at lower storey levels for the two considered load patterns (inverted TD and UD), which almost leads to the same distribution of plasticity (Figure 5) and, consequently, TD and UD give a *q*-factor value almost in the same range.

6.2 Support type effect on the *q*-factor

The effect of support type on the *q*-factor is discussed here. The R_S- and R_μ-factors are obtained for XBFs for a maximum value of λ_1 = 1.93 with pinned supports (λ_1 = 1.93) and fixed supports (λ_1’ = 1.93). For all frames, the capacity curves clearly show that, the greatest values of ultimate strength V_u and ultimate displacement Δ_u are obtained for XBFs with fixed supports.

In Fig. 8, it can be observed that the R_S- and R_μ-factors are greatly influenced by the type of support. In particular, the greatest values of R_S-factor are obtained for XBF structures with fixed supports. On the contrary, the R_μ-factor values of XBF structures with fixed supports turn out to be smaller than those of XBF structures with pinned supports. This is due to the fact that, change in the boundary conditions as column support type has an effect directly on the theory of dissipation energy of the structural system (plastic hinges distribution). In other words, each change in boundary conditions (support type) causes a change in the stiffness of the structure and, consequently influences the values of R_S- and R_μ-factors. Furthermore, the *q*-factor is little sensitive to the type of support. The *q*-factor value for XBF structures with fixed supports turns out to be almost the same as that for XBFs with pinned supports under the two considered lateral load pattern distributions (TD and UD).

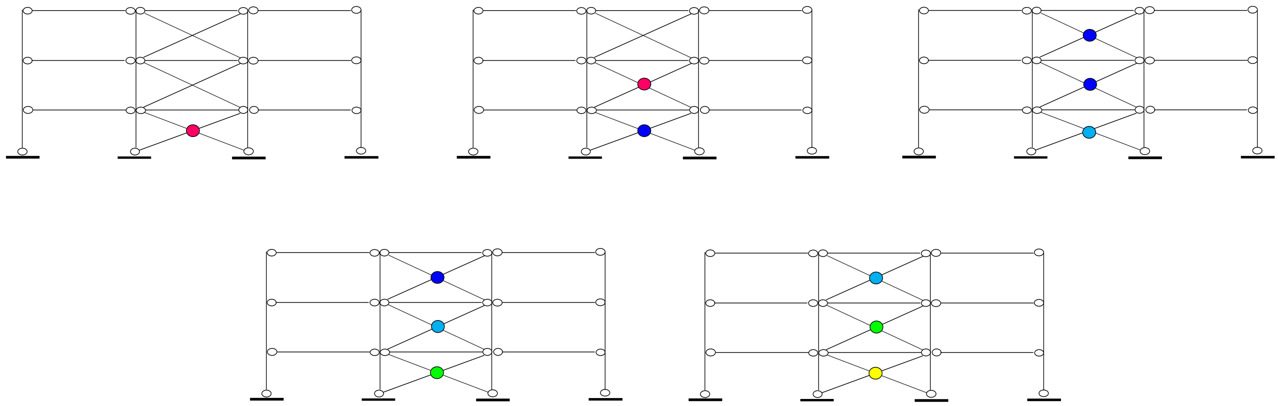

Figure 7: Deformation in time of three-storey frame with $\lambda_1 = 1.93$ under TD.

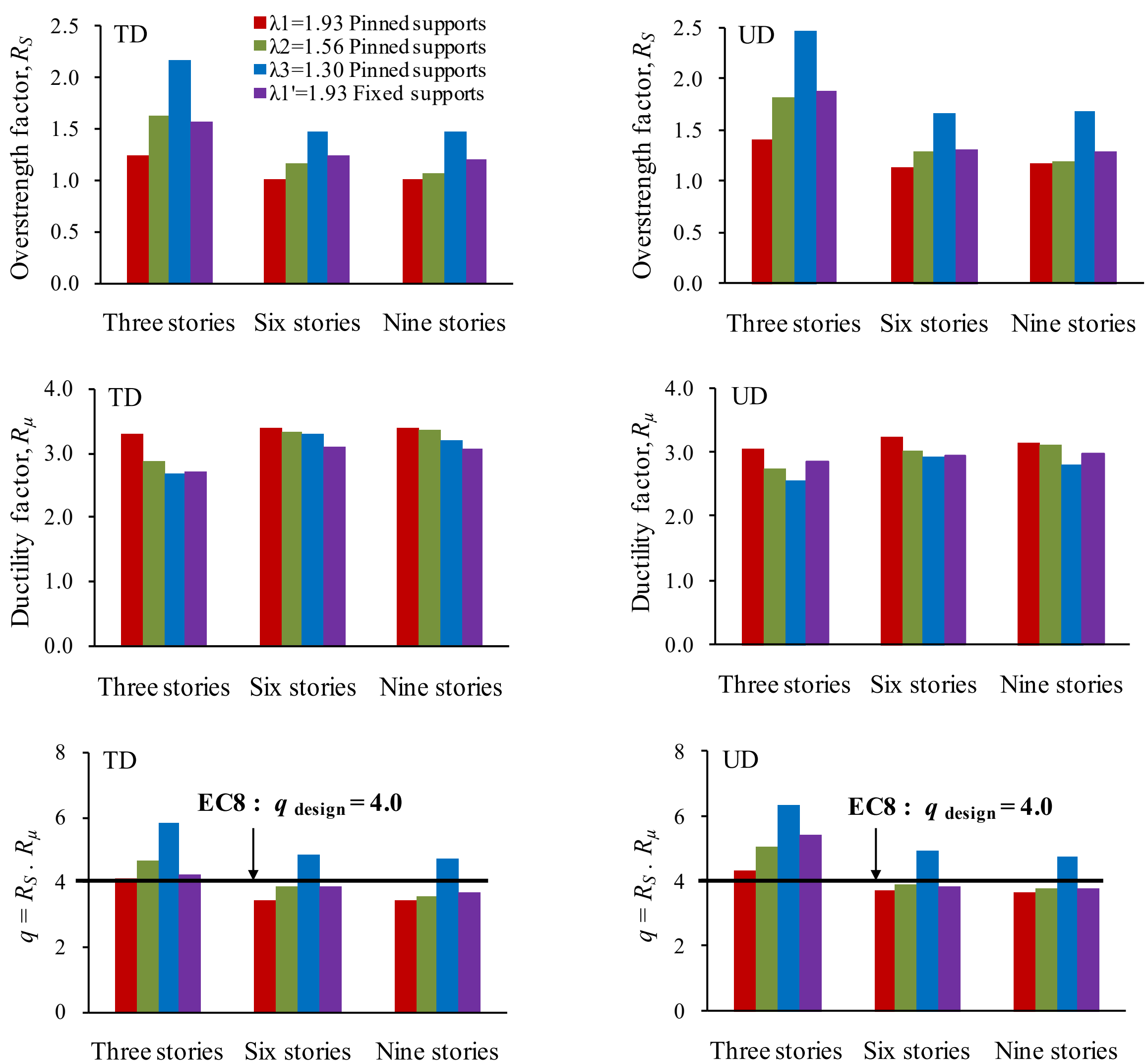

Figure 8: Behavior factor of the studied frames.

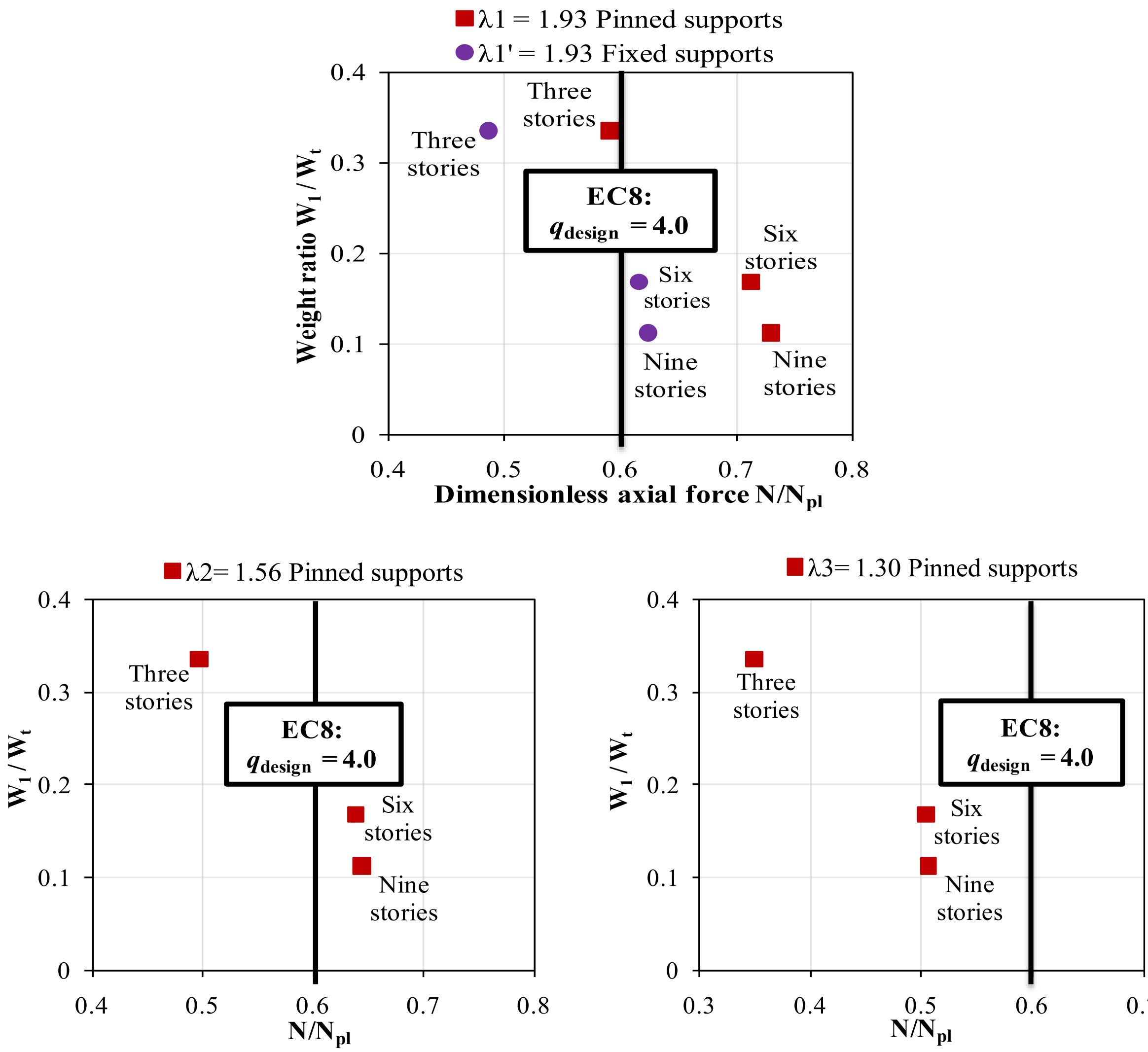

Figure 9: Behavior factor of the studied frames.

6.3 Brace slenderness ratio effect on the *q*-factor

In order to study the effects of brace slenderness ratio, λ_i, on the q-factor value, three different values of λ_i (λ_1 = 1.93, λ_2 = 1.56, and λ_3 = 1.30) are considered for each frame corresponding to the number of stories (three, six or nine stories) (see Table 1). Thus, R_S- and R_μ-factors are calculated for the three considered values of λ_i.

The variation of q-factor and its components as a function of brace slenderness ratio is given in Fig. 8. It can be observed that the R_S-factor is greatly influenced by the brace slenderness ratio. In particular, the lowest values of R_S-factor are obtained for the maximum value of the brace slenderness ratio (λ_1 = 1.93). However, the highest values of R_S-factor are obtained for the minimum value of the brace slenderness ratio (λ_3 = 1.30). This is due to the increase in the dimensions of braces' cross sections, allowing an increase of their plastic axial capacity N_{pl}. The value of R_μ-factor is little sensitive to the brace slenderness ratio, which is almost constant for six- and nine-storey frames. For three-storey frames, a decrease in the brace slenderness ratio value decreases the value of R_μ-factor.

In Fig. 8, the q-factors of the studied XBF structures considering the brace slenderness ratio effect are compared to the q-factor value specified by EC8. It is clear that the q-factor increases as the brace slenderness ratio decreases. For three-storey frames, the q-factors turn out to be larger than 4, which is prescribed in EC8, and for six- and nine-storey frames, only the structures designed with brace slenderness ratio λ_3 = 1.30 have q-factors larger than the EC8-specified value.

Fig. 9 shows the effect of the axial force ratio (N/N_{pl}) and the weight ratio (W_1/W_t) on the variation of *q*-factor. The axial force ratio represents the axial force (loading) N to the plastic axial capacity N_{pl} of first braces' sections that reach their ultimate load capacity (FS-B), and the weight ratio represents the weight of the first-storey W_1 to the total weight of the frame W_t. It is observed that the *q*-factor is strongly influenced by the value of the axial force ratio. As the number of stories increases, the axial force at the sections of FS-Bs increases (hence resulting in an increase in the total weight of the frame, W_t, compared to the weight of the first storey, W_1). This causes a local failure of FS-B sections (mechanism of soft storey), leading to limit the ductility of the frame. It imposes a reduction on the overstrength factor, consequently decreasing the *q*-factor value.

On the basis of the above results, the studied XBF structures present a weak point in their lateral strength. In fact, this structural typology is not able to provide sufficient resistance as far as the height of the structures or the axial force increases. As it has already been pointed out, the *q*-factor of the studied XBF structures is significantly influenced by the local response of braces' sections. For this reason, a criterion related to the local strength of braces' sections (N/N_{pl} < 0.60) has been proposed based on the results of these investigations. The main aim of the proposed criterion is to avoid the overestimation of the *q*-factor value and to optimize the agreement between the actual *q*-factor value and that specified in EC8.

In Fig. 9, the calculated *q*-factors for the studied XBF structures with different values of the axial force ratio are compared with the EC8-specified value. For medium- and high-rise frames, the result shows that the *q*-factor increases gradually with a decrease of the axial force ratio and, consequently, avoids the risk of overestimation of the *q*-factor value in the design. This result explicitly confirms the efficiency of the proposed criterion on the *q*-factor value.

7 Conclusions

A detailed study concerning the XBFs designed according to the European codes (EC3 and EC8) has been conducted. In this context, the effects of structural characteristics, brace slenderness ratio, and type of support are considered. The partial components (overstrength R_S and ductility R_μ) of the behavior factor (*q*-factor) are evaluated using NSPA with two load patterns (inverted TD and UD). On the basis of the previous results, the following conclusions can be drawn:

1. Overstrength R_S, ductility R_m, and behavior *q*-factors are strongly dependent on the structural characteristics of building. However, these factors are little sensitive to the lateral load patterns.
2. When the number of stories increases, the axial force at the FS-B sections increases. This leads to premature failure of these braces. Thus, the values of the R_S- and R_μ-factors decrease, which consequently reduces the value of *q*-factor.
3. The triangular and the uniform lateral load distributions give a *q*-factor almost in the same range.
4. The R_S- and R_μ-factors are greatly influenced by the type of support. In particular, the greatest values are obtained for XBFs with fixed supports. On the contrary, for the R_μ-factor, the greatest values are obtained for XBFs with pinned supports.
5. The *q*-factor is little sensitive to the support type. The *q*-factor value for XBFs with fixed supports turns out to be almost the same as that for XBFs with pinned supports.
6. The brace slenderness ratio λ_i makes a major difference in terms of *q*-factor, where a decrease in brace slenderness ratio increases the value of *q*-factor.
7. For the studied structures, EC8 gives a constant value of the *q*-factor. However, the obtained *q*-factors have different values for slenderness ratio and stories number.
8. Based on the ultimate limit capacity (using FEM-356 limits on member rotation capacity), the EC8 overestimates the *q*-factor, which leads to the potentially dangerous underestimation of the design base shear force.
9. A local strength criterion based on the control of axial force level and related to the local response of brace sections has been proposed to avoid the overestimation of *q*-factor value. So, when the proposed local strength criterion is satisfied, the resultant *q*-factor of the XBF structure is greater than 4.0.
10. The results of this study confirm the importance of the special rule given in EC8, which requires using overstrength factor in the design of brace to ensure homogeneous dissipative behavior of braces along the height of a structure.

As a final note, it is worth emphasizing that the results presented in this study are based on the NSPA performed on XBFs with three, six, and nine stories. Therefore, further research considering other parameters (taller structures) by means of nonlinear dynamic analysis is necessary for generalizing the presented conclusions.

References

[1] European Committee for Standardization. (2005). Eurocode 8: Design of structures for earthquake resistance-Part 1: General rules, seismic actions and rules for buildings. EN 1998-1-1. Brussels.

[2] UBC Standards. (1997). Volume 2 of the Uniform Building Code: Structural engineering design provisions. UBC97. Whittier.

[3] Louzai, A. & Abed, A. (2015). Evaluation of the seismic behavior factor of reinforced concrete frame structures based on comparative analysis between non-linear static pushover and incremental dynamic analyses. *Bulletin of Earthquake Engineering*, 13 (6), 1773-1793. DOI:10.1007/s10518-014-9689-7.

[4] Elghazouli, A. Y. (2010). Assessment of European seismic design procedures for steel framed structures. *Bulletin of Earthquake Engineering*, 8 (1), 65-89. DOI:10.1007/s10518-009-9125-6.

[5] Ferraioli, M., Lavino, A. & Mandara, A. (2014). Behaviour Factor of Code-Designed Steel Moment-Resisting Frames. *International Journal of Steel Structures*, 14 (2), 243–254. DOI:10.1007/s13296-014-2005-1.

[6] Balendra, T. & Huang, X. (2003). Overstrength and Ductility Factors for Steel Frames Designed According to BS 5950. *Journal of Structural Engineering ASCE*, 129 (8), 1019–1035. DOI: http://dx.doi.org/10.1061/(ASCE)0733-9445(2003)129:8(1019).

[7] Kim, J. & Choi, H. (2005). Response modification factors of chevron-braced frames. *Engineering Structures*, 27 (2), 285-300. DOI:10.1016/j.engstruct.2004.10.009.

[8] Mahmoudi, M. & Zaree, M. (2010). Evaluating response modification factors of concentrically braced steel frames. *Journal of Constructional Steel Research*, 66 (10), 1196-1204. https://doi.org/10.1016/j.jcsr.2010.04.004.

[9] Faggiano, B., Antonio Formisano, L. F., Macillo, V., Castaldo, C. & Mazzolani, F. M. (2014). Assessment of the Design Provisions for Steel Concentric X Bracing Frames with Reference to Italian and European Codes. *The Open Construction and Building Technology Journal*, 8 (Suppl 1: M3), 208-215. http://dx.doi.org /10.2174/1874836801408010208.

[10] Fanaie, N. & Shamlou, S. O. (2015). Response modification factor of mixed structures. *Steel and Composite Structures, An International Journal*, 19 (6), 1449-1466. DOI: 10.12989/scs.2015.19.6.1449.

[11] Kheyrodin, A. & Mashadiali, N. (2018). Response modification factor of concentrically braced frames with hexagonal pattern of braces. *Journal of Constructional Steel Research*, 148, 658–668. https://doi.org/10.1016/j.jcsr.2018.06.024.

[12] European Committee for Standardization. (2005). Eurocode 3: Design of steel structures-Part 1: General rules and rules for buildings. EN 1993-1-1. Brussels.

[13] Azad, S. K., Topkaya, C. & Astaneh-Asl, A (2017). Seismic behaviour of concentrically braced frames designed to AISC341 and EC8 provisions. *Journal of Constructional Steel Research*, 133, pp. 383-404. https://doi.org/10.1016/j.jcsr.2017.02.026.

[14] Ostraas, J. D., & Kraeinkler, H. (1990). *STRENGTH AND DUCTILITY CONSIDERATIONS IN SEISMIC DESIGN*. The John A. Blume Earthquake Engineering Center, Department of Civil and Environmental Engineering, Stanford University, California, USA. (Report No.90).

[15] Rahgozar, M. A. & Humar, J. L. (1998). Accounting for overstrength in seismic design of steel structures. *Canadian Journal of Civil Engineering*, 25 (1), 1–15. DOI: 10.1139/l97-045.

[16] Fanaie, N. & Afsar Dizaj, E. (2014). Response modification factor of the frames braced with reduced yielding segment BRB. *Structural Engineering and Mechanics, An International Journal*, 50 (1), 1-17. DOI: 10.12989/sem.2014.50.1.001.

[17] Attia, W. A. & Irheem, M. M. M. (2018). Boundary condition effect on response modification factor of X-braced steel frames, HBRC Journal, 4 (1), pp. 104-121. https://doi.org/10.1016/j.hbrcj.2016.03.002.

[18] Kappos, A. J. (1999). Evaluation of behaviour factors on the basis of ductility and overstrength studies. *Engineering Structures*, 21 (9), 823-835. DOI: http://dx.doi.org/10.1016/S0141-0296(98)00050-9.

[19] Mazzolani, F. M. & Piluso, V. (1996). *Theory and Design of Seismic Resistant Steel Frames*. London: E & FN Spon, An imprint of Chapman & Hall.

[20] ATC Standards. (1995). Applied Technology Council: A critical review of current approaches to earthquake-resistant design. ATC-34. Redwood City.

[21] Abdollahzadeh, G. & Banihashemi, M. (2013). Response modification factor of dual moment-resistant frame with buckling restrained brace (BRB). *Steel and Composite Structures, An International Journal*, 14 (6), 621-636. DOI: 10.12989/scs.2013.14.6.621.

[22] Yahmi, D., Branci, T., Bouchaïr, A. & Fournely, E. (2018). Evaluating the Behaviour Factor of Medium Ductile SMRF Structures. *Periodica Polytechnica Civil Engineering*, 62 (2), 373-385. https://doi.org/10.3311/PPci.10419.

[23] Dehghani, E., Hamidi, S. A., Tehrani, F. M., Goyal, A., Mirghaderi, R. (2015). New Practical Approach to Plastic Analysis of Steel Structures. *Periodica Polytechnica Civil Engineering*, 59 (1), 27-35. https://doi.org/10.3311/PPci.7578.

[24] Nassar, A., & Krawinkler, H. (1991). *Seismic demands for SDOF and MDOF systems*. The John A. Blume Earthquake Engineering Center, Department of Civil and Environmental Engineering, Stanford University, California, USA. (Report No. 95).

[25] Fajfar, P. (2000). A nonlinear analysis method for performance based seismic design. *Earthquake Spectra*, 16 (3), 573–592. DOI: http://dx.doi.org/10.1193/1.1586128.

[26] Mahmoudi, M. & Zaree, M. (2013). Determination the response modification factors of buckling restrained braced frames. *Procedia Engineering*, 54, 222-231. DOI:10.1016/j.proeng.2013.03.020.

[27] Yahmi, D., Branci, T., Bouchaïr, A. & Fournely, E. (2017). Evaluation of behaviour factors of steel moment-resisting frames using standard pushover method. *Procedia Engineering*, 199, 397-403. https://doi.org/10.1016/j.proeng.2017.09.130.

[28] Farshid, F. & Sepideh, R. (2020). Supervised probabilistic failure prediction of tuned mass damper-equipped high steel frames using machine learning methods. *Studia Geotechnica et Mechanica*, 42(3), 179–190. https://doi.org/10.2478/sgem-2019-0043.

[29] Kamaris, G. S., Vallianatou, Y. M. & Beskos, D. E. (2012). Seismic damage estimation of in-plane regular steel moment resisting and x-braced frames. *Bulletin of Earthquake*

Engineering, 10 (6), 1745-1766. DOI: 10.1007/s10518-012-9387-2.

[30] Computers and Structures Inc. (CSI). (2010). Structural Analysis Program: Linear and nonlinear static and dynamic analysis of three-dimensional structures. SAP2000. Berkeley.

[31] Mondal, A., Ghosh, S. & Reddy, G. R. (2013). Performance-based evaluation of the response reduction factor for ductile RC frames. *Engineering Structures*, 56, 1808–1819. DOI: http://dx.doi.org/10.1016/j.engstruct.2013.07.038.

[32] Federal Emergency Management Agency. (2000). American Society of Civil Engineers: Prestandard and Commentary for the Seismic Rehabilitation of Buildings. FEMA 356. Washington.

[33] Gholipour, M. & Alinia, M. M. (2016). Considerations on the Pushover Analysis of Multi-Story Steel Plate Shear Wall Structures. *Periodica Polytechnica Civil Engineering*, 60 (1), 113-126.https://doi.org/10.3311/PPci.7706.

[34] Branci, T., Yahmi, D. & BOUYAKOUB, S. (2020). ANALYSE STATIQUE NON LINÉAIRE D’OSSATURES MÉTALLIQUES CONTREVENTÉES PAR PALÉES EN X. *ALGÉRIE ÉQUIPEMENT*, 62, 01-07.

[35] Karavasilis, T. L., Bazeos, N. & Beskos, D. E. (2006). Maximum displacement profiles for the performance based seismic design of plane steel moment resisting frames. *Engineering Structures,* 28(1), 9–22. DOI: 10.1016/j.engstruct.2005.06.021.

[36] Banihashemi, M. R., Mirzagoltabar, A. R. & Tavakoli, H. R. (2015). Development of the performance based plastic design for steel moment resistant frame. *International Journal of Steel Structures*, 15 (1), 51-62. DOI: 10.1007/s13296-015-3004-6.

[37] Xiong, E., He, H., Cui, F. & Bai, L. (2016). Performance-Based Plastic Design Method for Steel Concentrically Braced Frames Using Target Drift and Yield Mechanism. *Periodica Polytechnica Civil Engineering*, 60 (1), 127-134. https://doi.org/10.3311/PPci.7383.

[38] Branci, T., Yahmi, D., Bouchaïr, A. & Fournely, E. (2016). Evaluation of Behavior Factor for Steel Moment-Resisting Frames. *International Journal of Civil and Environmental Engineering*, 10(3), 358-362. doi.org/10.5281/zenodo.1123588.